Proceedings of the ASME 2010 3rd Joint US-European Fluids Engineering Summer Meeting and
8th International Conference on Nanochannels, Microchannels, and Minichannels
FEDSM-ICNMM2010
August 1-5, 2010, Montreal, Canada

FEDSM-ICNMM2010-30797

THE EFFECT OF CHAOTIC MIXING ON HEAT TRANSFER IN CONTINUOUS THERMAL PROCESSES AT LOW PECLET NUMBERS

M.F.M. Speetjens
Laboratory for Energy Technology, Eindhoven
University of Technology, P.O. Box 513, 5600 MB
Eindhoven, The Netherlands

ABSTRACT
Chaotic fluid mixing is generally considered to enhance fluid-wall heat transfer and thermal homogenisation in laminar flows. However, this essentially concerns the transient stage towards a fully-developed (thermally-homogeneous) asymptotic state and then specifically for high Péclet numbers numbers *Pe* (convective heat transfer dominates). The role of chaos at lower *Pe* under both transient and asymptotic conditions, relevant to continuous thermal processes as e.g. micro-electronics cooling, remains largely unexplored to date. The present study seeks to gain first insight into this matter by the analysis of a representative model problem: heat transfer in the 2D time-periodic lid-driven cavity flow induced via non-adiabatic walls. Transient and asymptotic states are investigated in terms of both the temperature field and the thermal transport routes. This combined Eulerian-Lagrangian approach enables fundamental investigation of the connection between heat transfer and chaotic mixing and its ramifications for temperature distributions and heat-transfer rates. The analysis exposes a very different role of chaos in that its effectiveness for thermal homogenisation and heat-transfer enhancement is in low-*Pe* transient and asymptotic states marginal at best. Here chaos may in fact locally amplify temperature fluctuations and thus hamper instead of promote thermal homogeneity. These findings reveal that optimal thermal conditions are at lower *Pe* not automatic with chaotic mixing and may depend on a delicate interplay between flow and heat-transfer mechanisms.

1. INTRODUCTION

Laminar heat transfer is key to a wide variety of industrial processes of size extending from microns to meters. Examples range from the traditional mixing and thermal processing of viscous fluids [1-4] via compact processing equipment [5,6] down to emerging micro-fluidics applications [7-9]. Typical objectives are efficient fluid-wall heat transfer and rapid thermal homogenisation. The general consensus is that chaotic mixing is conducive to both ends. However, its exact role in thermal transport remains ill-understood to date, particularly in the essentially advective-diffusive regime at low Péclet numbers (*Pe*) that characterises emerging technologies as process intensification and micro-fluidics applications.[1] This motivates the present study, which seeks to further explore the role of chaos in thermal transport.

Studies on chaotic mixing in heat transfer concern primarily the transient stage towards a fully-developed (thermally-homogeneous) asymptotic state and then typically for higher *Pe*, where convection dominates (typically from $Pe=1000$ onwards). Here chaos indeed increases heat-transfer rates and thermal-homogenisation capacities by essentially reducing the duration or spatial extent of the transient stage [1,2,10-12]. However, analyses on the role of chaos in the asymptotic state - and then in particular for low *Pe* - are rare, despite its relevance to continuous thermal processes as e.g. micro-electronics cooling and compact fluids-engineering equipment. The present study aims at shedding first light on this matter by way of a comparative heat-transfer analysis in both transient and asymptotic states for low *Pe* (i.e. around $Pe\sim100$).

The well-known two-dimensional (2D) lid-driven cavity flow serves as case study for the present analysis. The flow is driven by steady or time-periodic motion of adiabatic side

[1] Some terminology: advection is transport by fluid motion; diffusion is transport by molecular motion. For heat transfer problems, advection and diffusion are usually denoted “convection” and “conduction,” respectively. Generic laminar transport involves both transport mechanisms; mixing is transport by advection only.

walls; thermal transport is induced by a temperature differential between bottom (hot) and top (cold) walls. The system may thus accommodate steady and time-periodic asymptotic states. Fluid motion and heat transfer are governed by the full conservation laws including viscous and inertial effects (i.e. non-zero Reynolds number *Re*). Past studies have shown that this configuration admits chaotic advection in the Stokes limit *Re=0* [13]. Thus the case study constitutes a simplified yet realistic representation of practical heat-transfer problems.

Heat transfer is investigated from both an Eulerian and a Lagrangian perspective. The former leans on eigenmode decomposition of the evolution of the temperature field [2,10,12]; the latter on representation of thermal transport as the "motion" of a "fluid." This fluid-motion analogy admits heat-transfer analyses by well-established Lagrangian methods from laminar-mixing studies and enables fundamental investigation of the connection between heat transfer and chaotic mixing [14,15]. The study concentrates on the role of chaos in heat-transfer enhancement and thermal homogenisation in the transient and asymptotic states.

The exposition is organised as follows. Section 2 introduces the model problem and Eulerian and Lagrangian approaches towards thermal analyses. Mixing is examined in Section 3. The heat-transfer analysis is discussed in Section 4. Conclusions are in Section 5.

2. MODEL PROBLEM AND METHODOLOGY

2.1 Fluid motion and heat transfer

Considered is the fluid flow and heat transfer inside a 2D non-dimensional rectangular cavity (unit width and height *D*). The flow is driven by translating adiabatic side walls with velocities $v_l = \cos^2(\pi t/\tau) \geq 0$ (left) and $v_r = -\sin^2(\pi t/\tau) \leq 0$ (right) for steady (τ=0) and time-periodic (τ>0) conditions. Heat transfer is set up by maintaining the top and bottom sides of the finite-thickness (ΔD) horizontal cavity walls at temperatures *T=0* and *T=1*, respectively. Fluid motion is, omitting buoyancy, governed by

$$\nabla \cdot \vec{u} = 0\,, \quad \mathrm{Re}\left[\frac{\partial \vec{u}}{\partial t} + \vec{u}\cdot\nabla\vec{u}\right] = -\nabla p + \nabla^2 \vec{u}\,, \tag{1}$$

and heat transfer inside flow region and solid walls is governed by

$$\frac{\partial T}{\partial t} + \vec{u}\cdot\nabla T = \frac{1}{Pe}\nabla^2 T\,, \qquad \frac{\partial T}{\partial t} = \frac{1}{Pe_s}\nabla^2 T\,, \tag{2}$$

respectively, completed by boundary conditions as described above and initial condition $T(\vec{x},0)=0$. The corresponding non-dimensional parameters read $D=H/L$, $\Delta D=\Delta H/L$, $Re=UL/\nu$, $Pe=UL/\alpha$, $\tau=UT_f/L$, $\Lambda=\lambda_s/\lambda\,\alpha$ and $Pe_s=UL/\alpha_s$. with (*L,H*) width and height of the physical cavity, ΔH thickness of the non-adiabatic walls, *U* the forcing velocity and T_f the corresponding period time, ν the kinematic viscosity and (λ ,α) the thermal conductivity and thermal diffusivity (subscript "s" indicates non-adiabatic wall). Figure 1 gives a schematic of the non-dimensional configuration. Here only heat transfer in the flow domain is considered as a function of the non-dimensional period time τ; the remaining parameters are fixed at *D=1*, ΔD *=0.2*, *Re=1*, *Pe=100,* Pe_s*=1* and Λ*=1*. The flow and temperature fields are simulated by the commercial CFD package Fluent.

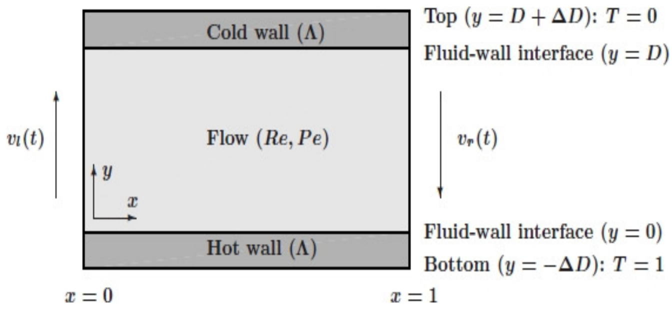

Figure 1. Non-dimensional problem definition.

2.2 Methods for heat-transfer analysis

Eulerian approach The spatio-temporal evolution of the temperature field in the flow region, governed by (2), is dictated by the eigenmodes of the advection-diffusion operator [2,10,12]. The eigenmode decomposition of the temperature field reads

$$T(\vec{x},t) = \sum_{m=0}^{\infty} C_m h_m(\vec{x},t)\,, \qquad h_m(\vec{x},t) = e^{\mu_m t}\psi_m(\vec{x})\,, \tag{3}$$

with $h_m(\vec{x},t)$ the eigenmodes. The temporal and spatial properties of these eigenmode are determined by the corresponding (complex) eigenvalues μ_m and eigenfunctions $\psi_m(\vec{x})$, respectively. Finite *Pe* restricts the eigenvalues to $\mathrm{Re}(\mu_m) \leq 0$ for all *m* [10]. This has two important implications. First, the temperature field always evolves towards an asymptotic state $T_\infty(\vec{x},t) \equiv \lim_{t\to\infty} T(\vec{x},t) = \sum C_m h_m^0(\vec{x},t)$, with $h_m^0(\vec{x},t)$ the eigenmodes h_m for which $\mathrm{Re}(\mu_m)=0$. Second, this evolution, after a short-lived initial stage, is dominated by the slowest-decaying eigenmodes, that is, modes $h_m^d(\vec{x},t)$ associated with eigenvalues μ_m^d having identical $\mathrm{Re}(\mu_m^d)=\mu_d$, with $\mu_d = \max[\mathrm{Re}(\mu_m)] < 0$. This implies that the temperature field rapidly collapses on the form

$$T(\vec{x},t) = e^{-t/\tau_d}\Psi(\vec{x},t) + T_\infty(\vec{x},t)\,,$$
$$\Psi(\vec{x},t) = \sum C_m e^{\mathrm{Im}(\mu_m^d)t}\psi_m(\vec{x})\,, \tag{4}$$

with $\Psi(\vec{x},t)$ the transient mode and $\tau = -1/\mu_d$ its corresponding decay time.

Lagrangian approach Key to the Lagrangian concept by [14,15] is that heat transfer happens along paths ("thermal trajectories") delineated by the total heat flux. These thermal trajectories $\vec{x}_T$ are in the flow region described by

$$\frac{d\vec{x}_T}{dt}=\vec{v}, \qquad \frac{\partial T}{\partial t}+\nabla\cdot\left(T\vec{v}\right)=0, \tag{5}$$

with $\vec{v}=\vec{u}-Pe^{-1}\nabla(\ln T)$, and are the thermal analogy to the Lagrangian fluid trajectories, governed by

$$\frac{d\vec{x}}{dt}=\vec{u}, \qquad \frac{\partial \rho}{\partial t}+\nabla\cdot\left(\rho\vec{u}\right)=0, \tag{6}$$

This exposes T, $\vec{v}$ and $\vec{x}_T$ as the thermal analogies to the fluid density ρ, fluid velocity $\vec{u}$ and fluid trajectories $\vec{x}$ and thus enables representation of heat transfer entirely in terms of the "motion" of a "fluid" subject to continuity. This admits heat-transfer analyses by well-established Lagrangian methods from laminar-mixing studies [16,17]. These methods lean on the property that continuity "organises" fluid trajectories $\vec{x}$ into sets of coherent structures ("flow topology") that geometrically determine the fluid transport. The thermal trajectories $\vec{x}_T$, by virtue of the fluid-motion analogy, form a thermal topology of essentially equivalent composition. Topological analysis of this thermal topology offers promising new thermal-analysis capabilities. The flow and thermal topologies are determined by numerical post-processing of the simulated flow and temperature fields by dedicated software implemented in the high-level programming language Matlab and based on methodologies described in [15].

3. MIXING CHARACTERISTICS

The present study concentrates specifically on the role of chaotic advection in thermal transport. Chaos can in 2D systems be accomplished only by unsteady effects, here introduced by time-periodic forcing by the vertical sidewalls. For the present low-Reynolds flow (*Re=1*) this external periodicity is imparted on the internal flow: $\vec{u}(\vec{x},t)=\vec{u}(\vec{x},t+\tau)$. Furthermore, simulations reveal that the flow field, in comparison to the temperature field (Section 4.2), reaches its asymptotic time-periodic state almost instantly on grounds of the negligible fluid inertia and the absence of coupling by buoyancy and temperature-dependent fluid properties. Hence, for mixing characteristics only the asymptotic flow state is relevant.

The steady flow topology ($\tau=0$) coincides with the streamline portrait shown in Figure 2(a) and consists entirely of closed streamlines defining recirculation zones ("islands"), signifying absence of any mixing. The time-periodic flow topology can be visualised by Poincaré-sections (subsequent positions of passive tracers at time levels t=[0,τ,2τ,...]) [16]. The Poincaré-sections of passive tracers released at "strategic" locations visualise the flow topology similar to the streamline portraits in steady flows.

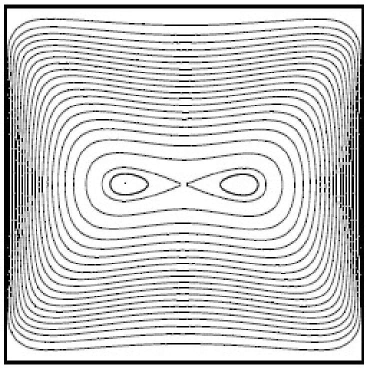

(a) Steady flow (τ=0)

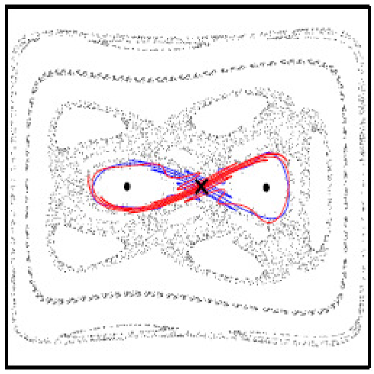

(b) Time-periodic flow (τ=3)

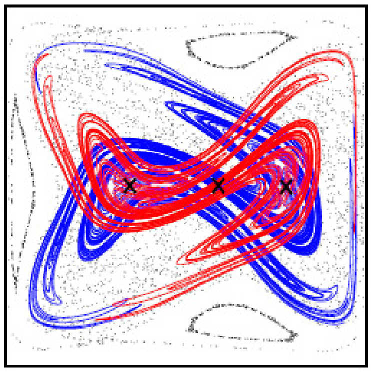

(c) Time-periodic flow (τ=5)

Figure 2. Flow topology versus period time τ. Steady flow: streamlines; time-periodic flow: Poincaré-sections of passive tracers released on the line y=0.5. Red/blue curves indicate manifolds in the chaotic sea; crosses indicate their origin.

Figures 2(b)-(c) show the Poincaré-sections (black dots) of passive tracers released on the line *y=0.5 in* time-periodic flows (τ*>0)*, disclosing two kinds of coherent structures: (i) chaotic sea; (ii) islands embedded in the chaotic sea. The chaotic sea is an essentially unsteady phenomenon that ensues from disintegration of (parts of) islands; the remaining islands are remnants of their (partially-disintegrated) steady-state counterparts [16]. The red and blue curves within the sea delineate the principal transport directions upon progression and regression in time, respectively, and are its underlying coherent structures. These curves (termed "manifolds") effectuate chaotic advection and are key to the accomplishment of "efficient mixing" [16,17].[2] (Filled circles and crosses indicate centres of islands and origins of manifolds, respectively.) Visualisation of the flow topology thus directly exposes the poor and good mixing zones. Stronger time-periodicity (increasing τ) improves mixing, though (localised) non-mixing zones persist. This is consistent with the findings on the Stokes limit *Re=0* [13].

4. HEAT-TRANSFER ANALYSIS

4.1 Introduction

Figure 3 gives the evolution of the temperature field towards its time-independent asymptotic state $T_\infty(\vec{x})$ in case of steady forcing. Clearly visible is the penetration of the higher-temperature zone from the hot bottom wall into the interior of the domain until the final state in panel (d) is attained. Shown evolution demonstrates that the temperature field, in contrast to the fluid motion (Section 3), undergoes a significant transient phase before reaching its asymptotic state. The evolutions corresponding with time-periodic flow forcings for $\tau=3$ and $\tau=5$ are similar to that of the steady case in that temperature distributions and significance of the transient are comparable. Time-periodicity in fact manifests itself in weak fluctuations of the temperature field around a mean state that is nearly indistinguishable from the steady-forcing case. Moreover, effects of flow forcing seem to be restricted predominantly to the interior of the flow domain. These issues are investigated further hereafter.

4.2 Eulerian analysis

The transient behaviour is demonstrated in Figure 4 in terms of the spatially-averaged departure of the temperature field from its asymptotic state: $\Delta T(t)=\iint[T(\vec{x},t)-T_\infty(\vec{x},t)]dxdy$. The evolutions clearly exhibit an exponential decay in time, implying that the temperature field indeed obeys the form (4). Moreover, the evolutions virtually coincide, meaning that decay rates are practically insensitive to variations in flow forcing and degree of chaos. The corresponding decay times amount to $\tau_d=17.1$ for steady forcing and $\tau_d=16.5$ and $\tau_d=17.0$ for time-periodic forcing at $\tau=3$ and $\tau=5$, respectively. Comparison with the diffusion-only decay time $\tau_\alpha=Pe(H_*/\pi)^2=19.86$, with $H_*=D+2\Delta D$, reveals that advection in itself, notwithstanding the apparent irrelevance of degree of chaos, accelerates the transient. These findings are consistent with studies in [10,12], which established that chaos becomes effective for transient acceleration only for sufficiently high *Pe*. Lower *Pe* diminishes if not completely negates the effect of chaos. Estimates based on said studies, supported by results in [2], put forth *Pe~O(100-1000)* as range in which chaos can be expected to become a significant accelerant for the transient. The current system is at the lower end of this regime.

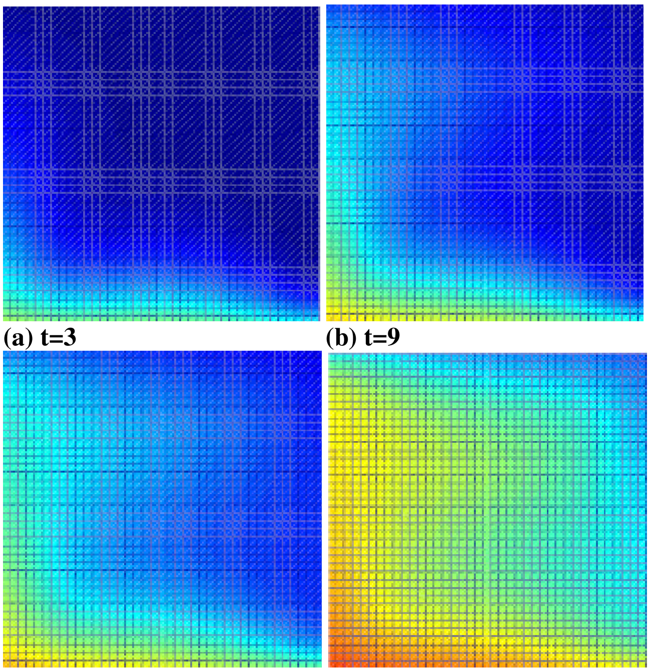

(a) t=3 **(b) t=9**

(c) t=15 **(d) Asymptotic state**

Figure 3. Temperature evolution for steady flow forcing.

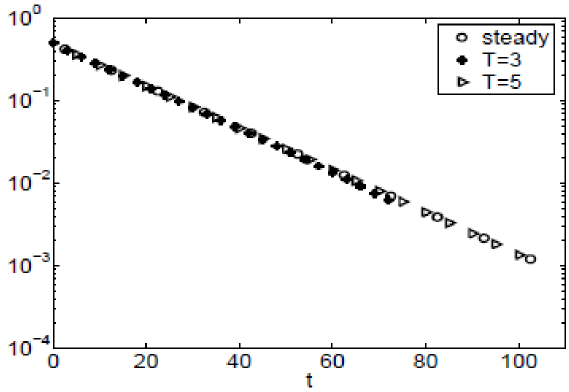

Figure 4. Decay of the mean departure $\Delta T(t)$.

Numerical simulations reveal that the transient (Ψ) and asymptotic (T_∞) modes are time-independent and time-periodic in case of steady and time-periodic forcing, respectively. Thus the temperature evolutions rapidly lock in with the nature of the flow forcing. Figure 5 gives the transient modes for steady forcing at any time *t* in comparison to that of the time-periodic cases at the

[2] Manifolds densely fill the chaotic seas; here only part is shown.

time levels $t = k\tau$, exposing a strong similarity. Similarly, the time-periodic asymptotic states at $t = k\tau$ are in good agreement with that of the steady case shown in Figure 3(d).

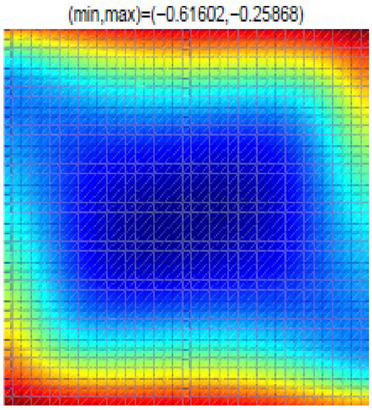

(a) Steady forcing for all t

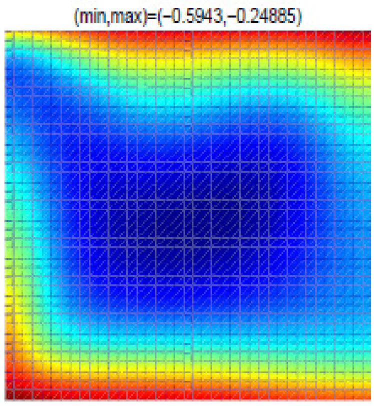

(b) Time-periodic forcing at $t = k\tau$ ($\tau = 3$)

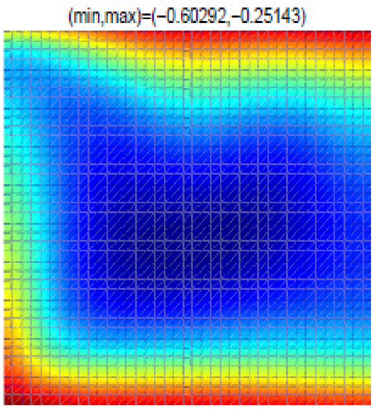

(c) Time-periodic forcing at $t = k\tau$ ($\tau = 5$)

Figure 5. Transient mode Ψ.

Primary difference between steady and time-periodic forcings are weak time-periodic fluctuations of the transient and asymptotic modes in the latter case. This implies eigenmode decompositions according to the Fourier expansions

$$T_\infty(\vec{x},t) \equiv \sum \tilde{T}_m(\vec{x}) e^{2\pi i m t/\tau}, \quad \Psi(\vec{x},t) \equiv \sum \tilde{\Psi}_m(\vec{x}) e^{2\pi i m t/\tau}, \qquad (7)$$

with $\tilde{T}_m$ and $\tilde{\Psi}_m$ the associated Fourier spectra [18].[3] Figure 6 gives the corresponding Fourier spectra in terms of the spatial averages $\overline{T}_m(t) = \iint |\tilde{T}_m(\vec{x})| dxdy$ and $\overline{\Psi}_m(t) = \iint |\tilde{\Psi}_m(\vec{x})| dxdy$. Shown Fourier spectra exhibit a rapid decay with growing wave number m (or frequency $f_m = m/\tau$), meaning that only low-frequency contributions are relevant to the evolution of the temperature fields. Decay rates are such that $\overline{T}_1/\overline{T}_0 \approx O(10^{-2})$ and $\overline{T}_m/\overline{T}_0 < O(10^{-2})$ for $m>1$ and likewise for $\overline{\Psi}_m$, meaning that modes $m=0,1$ dominate the evolution of both the transient and asymptotic modes. Hence, the temperature field throughout its entire evolution to good approximation is described by

$$\begin{aligned} T(\vec{x},t) &= e^{-t/\tau_d}[\tilde{\Psi}_0(\vec{x}) + 2\,\mathrm{Re}\{\tilde{\Psi}_1(\vec{x})e^{2\pi i t/\tau}\}] \\ &\quad + \tilde{T}_0(\vec{x}) + 2\,\mathrm{Re}\{\tilde{T}_1(\vec{x})e^{2\pi i t/\tau}\}, \end{aligned} \qquad (8)$$

comprising only the steady ($m=0$) and first oscillatory mode ($m=1$) of the Fourier expansions (7). This tremendously reduces the complexity of the eigenmode decomposition (3) yet without compromising its physical validity.

Fourier modes $\tilde{T}_0$ and $\tilde{\Psi}_0$ differ only marginally for $\tau = 3$ and $\tau = 5$ and closely resemble the associated asymptotic and transient modes, respectively. This implies that time-periodicity (and chaos) manifests itself predominantly in the emergence of Fourier modes $m=1$ against a basically invariable background state. The evolution of these modes through property $\mathrm{Re}[\tilde{f}_m(\vec{x})e^{2\pi i m t/\tau}] = \mathrm{Re}[\tilde{f}_m]\cos(2\pi m t/\tau) - \mathrm{Im}[\tilde{f}_m]\sin(2\pi m t/\tau)$ smoothly alternates between the respective real and imaginary parts. Figures 7 and show the real and imaginary contributions of the asymptotic and transient modes, respectively, for $\tau = 3$ and $\tau = 5$, exposing a string of peaks and valleys arranged around the centre of the domain that in essence set up a clockwise rotation of temperature waves. The asymptotic and transient modes correlate well in that regions accommodating peaks and valleys largely overlap. However, these features not necessarily coincide, meaning that, by virtue of constructive and destructive interference, interaction of asymptotic and transient modes results in both local damping and amplification of temperature fluctuations during the transient. This grows weaker as time progresses on account of the exponential decay of the transient mode, meaning that fluctuations diminish during evolution to the asymptotic state.

The above findings have important ramifications for fluid-wall heat-transfer enhancement and thermal homogenisation. Net fluid-wall heat transfer is proportional to the mean temperature

---

[3] Note that real temperature fields imply real modes $\tilde{T}_0$ and $\tilde{\Psi}_0$ and complex conjugate pairs $\tilde{T}_m = \tilde{T}^*_{-m}$ and $\tilde{\Psi}_m = \tilde{\Psi}^*_{-m}$ for modes |m|>0.

gradient at the non-adiabatic walls during each forcing cycle, which, due to the time periodicity of the temperature evolution (8), depends only on Fourier modes $\tilde{T}_0$ and $\tilde{\Psi}_0$. The fact that these modes are virtually insensitive to time-periodicity and variation of τ implies that temperature gradients depend primarily on the relative strength of advection (set by *Pe*) yet *not* on its nature. Hence, time-periodicity (and chaos) is in both transient and asymptotic states virtually ineffective as a means of fluid-wall heat-transfer enhancement.

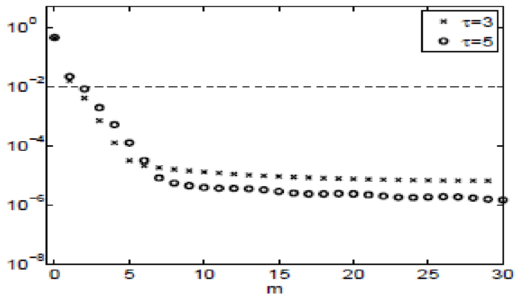

(a) Transient mode Ψ

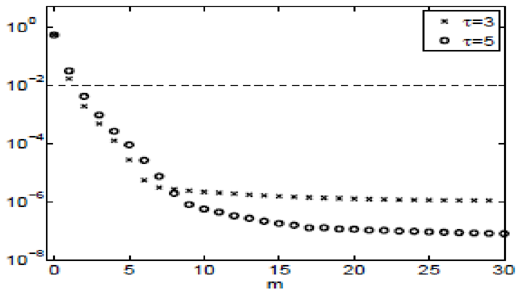

(b) Asymptotic mode T_∞

Figure 6. Fourier spectra of transient and asymptotic modes.

The dominance of Fourier modes *m=0* means that thermal homogenisation leans mainly on their spatial distribution and relative magnitude. The transient mode $\tilde{\Psi}_0$ (similar to Figure 5) is strongly heterogeneous in the entire domain, whereas the asymptotic mode $\tilde{T}_0$ (similar to Figure 3 (d)) has a sizeable internal region with approximately uniform state. Heterogeneity due to $\tilde{\Psi}_0$ decays exponentially during the transient, however. Furthermore, the above revealed that temperature fluctuations due to Fourier modes *m=1* also diminish during the transient. These properties imply that, overall, the temperature field becomes more homogeneous during the transient. Time-periodicity (and chaos), on the other hand, amplifies temperature fluctuations and thus promotes heterogeneity. Hence, thermal homogenisation is most pronounced in the asymptotic state and, remarkably, for steady flow forcing.

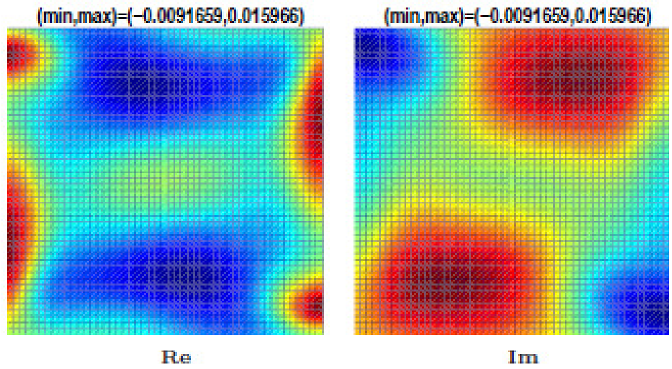

(a) $\tau = 3$

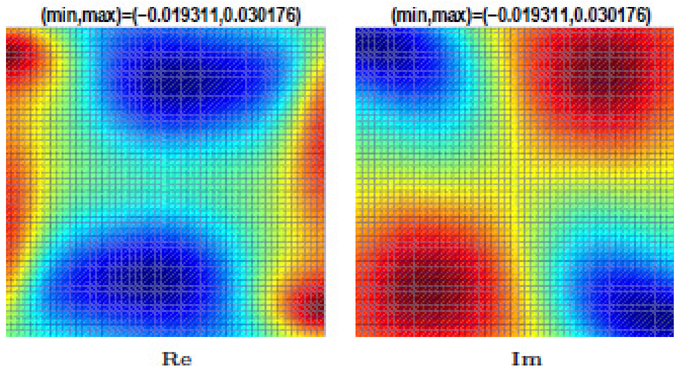

(b) $\tau = 5$

Figure 7. Fourier mode *m=1* for the asymptotic modes.

4.3 Lagrangian analysis

Heat transfer can be made visible in several ways: (instantaneous) thermal streamlines and thermal Poincaré-sections. Thermal streamlines and thermal Poincaré-sections visualise the transport routes of heat ("thermal topology") governed by (5) for steady and time-periodic conditions, respectively, in the same way as their fluid-motion analogies. Instantaneous thermal streamlines (ITSs) for unsteady conditions, on the other hand, delineate momentary heat fluxes and, strictly, do not coincide with the thermal topology. ITSs are nonetheless intimately related to the thermal topology and afford insight into its formation and composition.

Figure 9 gives the progression of the ITSs (panels (a)-(c)) during the transient and the associated asymptotic thermal streamline portrait (panel (d)) in case of steady flow forcing.

The asymptotic thermal topology comprises two distinct regions: (i) the thermal path (black), facilitating heat transfer from bottom to top wall; (ii) the thermal island (blue), entrapping thermal energy. (This thermal path in fact always exists in the presence of non-adiabatic walls [14,15].) The ITSs visualise the formation of this asymptotic state and its constituent coherent structures. The black curves delineate the uni-directional heat flux between the non-adiabatic walls; the red curves delineate the internal circulatory heat flux. Former and latter underly formation of the thermal path and thermal island, respectively, of the asymptotic state. Furthermore, instantaneous thermal islands, as highlighted in blue in Figure 9 (a), may sometimes emerge during the transient.

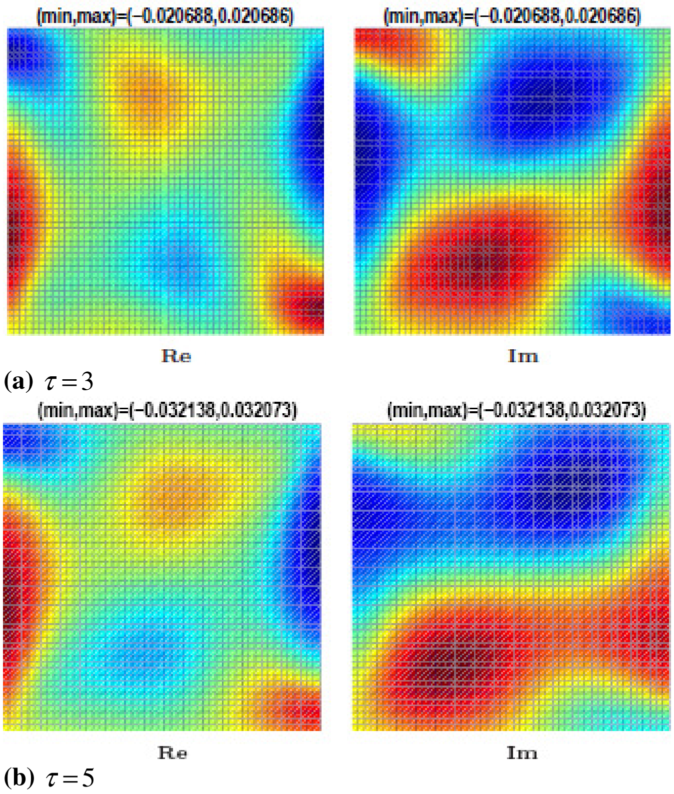

Figure 8. Fourier mode *m=1* for the transient modes.

Figure 10 gives the progression of the ITSs during the transient in case of time-periodic flow forcing with $\tau=3$. Left and right columns correspond with time levels $\tau=(k-1/2)\tau$ and $\tau=k\tau$, respectively, where *k=1,2,…*; panels (d) and (h) give the ITSs of the associated asymptotic states. The basic make-up is the same as for the steady case in that a similar arrangement of regions with uni-directional (black) and circulatory (red) heat flux occurs. Furthermore, instantaneous thermal islands emerge sporadically during the transient and persist in the asymptotic state (again highlighted in blue). Essential differences with the steady case are, first, absence of a fixed asymptotic thermal streamline portrait and, second, non-monotonic evolution of the ITSs. These are evident consequences of the time-periodicity.

The ITSs in the circulation zone are shaped by instantaneous stagnation points (i.e. points with $\vec{v}=\vec{0}$) and, if present, by separatrices that bound instantaneous thermal islands. ITSs are either attracted ($\nabla\cdot\vec{v}<\vec{0}$) or repelled ($\nabla\cdot\vec{v}>\vec{0}$) by such entities, in which cases the latter act as momentary heat sinks or heat sources, respectively. Attraction thus causes net heat flux into the area surrounding the instantaneous stagnation point and, by virtue of (5), rising local temperature $dT/dt=-T\nabla\cdot\vec{v}>\vec{0}$, where *d/dt* represents the material derivative relative to $\vec{v}$. Repulsion, conversely, causes a local temperature drop: $dT/dt=-T\nabla\cdot\vec{v}<\vec{0}$.

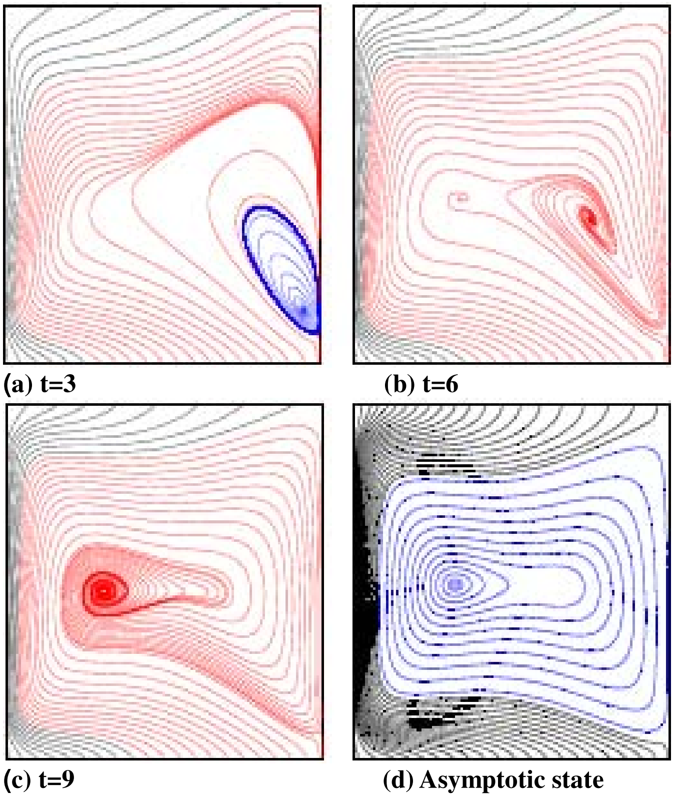

Figure 9. Instantaneous thermal streamlines (steady forcing).

The transient for steady forcing initially accommodates an attracting separatrix, bounding the instantaneous thermal island centred on a repelling instantaneous stagnation, which rapidly gives way to attracting instantaneous stagnation points (Figures 9 (a)-(c)). These attracting entities set up the circulatory heat influx (and associated temperature rise) in the flow interior that leads to the formation of the thermal island in the asymptotic state (Figure 9 (d)). The separatrices and instantaneous stagnation points emerging during the transient for the time-periodic forcing (Figure 10) lead to the asymptotic state in the same way as for the steady-forcing case. However, the separatrix/instantaneous stagnation point associated with the instantaneous thermal island of the asymptotic state exhibit essentially different behaviour by periodically alternating between attractor/repellor (Figure 10 (d)) and repellor/attractor (Figure 10 (h)). The former and latter situations correspond with periodic heat take-up from the hot bottom wall and heat rejection via the cold top wall, respectively.

Figure 11 visualises the asymptotic thermal topology for $\tau=3$ and $\tau=5$ by thermal Poincaré-sections. Two distinct regions can be distinguished. First, the thermal path (represented in time-averaged form by the gray curves) that sets up directional fluid-wall heat exchange. Second, thermal manifolds in the flow interior (red/blue curves) that accomplish chaotic heat transfer (or "thermal mixing") in essentially the same way as the manifolds in

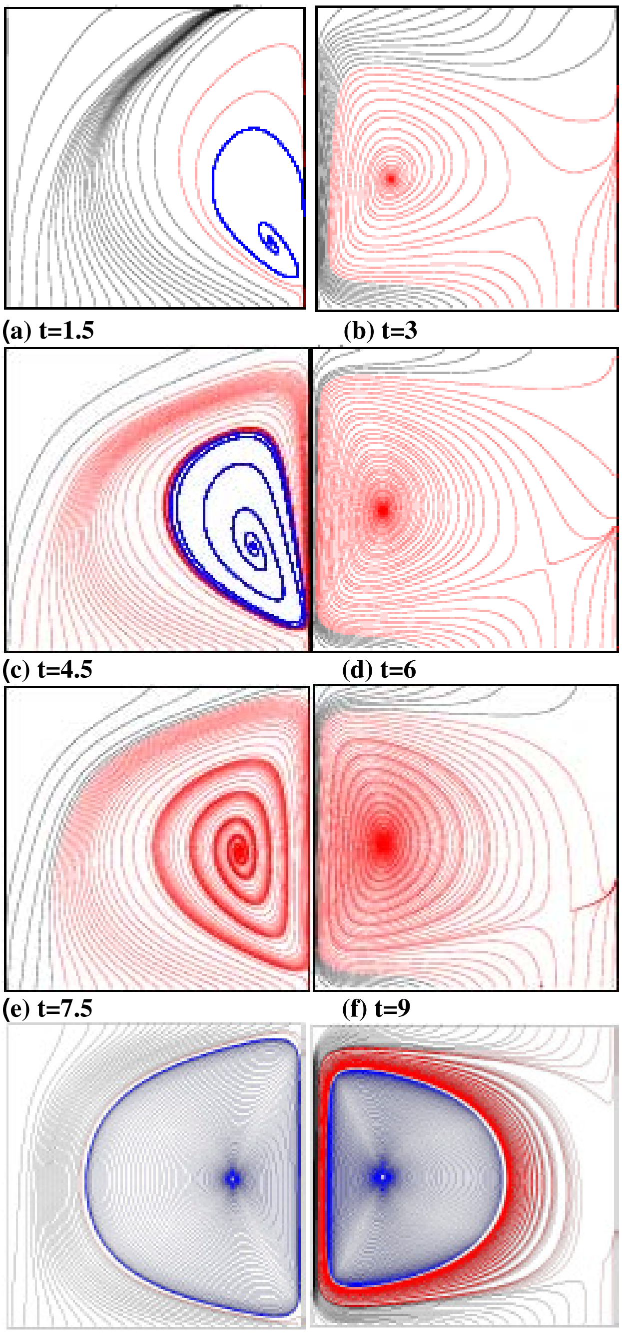

(a) t=1.5 (b) t=3 (c) t=4.5 (d) t=6 (e) t=7.5 (f) t=9 (g) $\tau=(k-1/2)\tau$ (h) $\tau=k\tau$

Figure 10. Instantaneous thermal streamlines for $\tau=3$.

Figure 2 accomplish chaotic advection (or fluid mixing). The expansion of the thermal manifolds with increasing τ nicely demonstrates the chaotisation of the interior heat transfer induced by stronger fluid mixing. The thermal path - and thus the fluid-wall heat exchange - remains essentially unaffected and contains the chaotic heat-transfer zone, though. This explains the ineffectiveness of fluid mixing for fluid-wall heat-transfer enhancement (Section 4.2).

The ITSs of both steady and time-periodic cases -- and then in particular large sections of the thermal path - rapidly assume a state closely resembling their corresponding asymptotic states, after which they slowly evolve towards the latter in an approximately self-similar manner. (Compare to this end the time instances in Figures 9 and 10 with the duration of the entire transient in Figure 4}.) This implies that the system quickly settles for a quasi-asymptotic state in which the thermal path has already largely been established and transient effects predominantly ensue from the relatively slow formation of the (instantaneous) thermal island of the asymptotic state. This formation thus determines the duration of the transient and said quasi-asymptotic state coincides well with the exponential and self-similar temperature decay described by the transient mode Ψ (Figure 4).

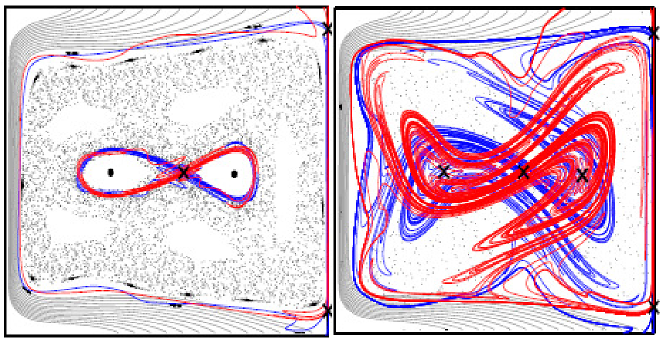

(a) $\tau=3$ (b) $\tau=5$

Figure 11. Thermal topology versus τ. Gray indicates time-averaged thermal path; red/blue indicates manifolds in the chaotic sea; crosses indicate their origin.

The thermal Poincaré-sections expose two families of manifolds (best visible in panel (a)): (i) outer manifolds originating from the right wall and enveloping the chaotic core; (ii) inner manifolds occupying the chaotic core. Both families become increasingly intertwined (and indistinguishable) with growing τ (panel (b)). The outer manifolds demarcate the roughly annular transition region between thermal path and chaotic zone and set up a clockwise heat circulation around the core of said zone by basically "dredging" through this area within the course of each period. This "dredging" happens with intermittent intensity, fluctuating stronger with increasing τ, thus amplifying temperature oscillations – and promoting heterogeneity - in the transition region. This explains the clockwise rotation of temperature waves around the domain centre. The inner manifolds accomplish strong chaotic heat transfer in the core region, thus maintaining relative thermal homogeneity there, and at the same time amplifying temperature fluctuations in the transition region. Hence, these manifolds play a dual role by promoting both thermal homogeneity and heterogeneity. This explains the clockwise rotation of temperature waves around the domain centre with intensity that grows stronger with increasing chaos, as observed in the Eulerian analysis.

5. CONCLUSIONS

The study investigates the role of chaotic advection in laminar heat transfer for low Péclet numbers Pe for two issues of great practical relevance: (i) heat-transfer enhancement; (ii) thermal homogenisation. To this end heat transfer in the well-known 2D lid-driven cavity is examined for both steady and time-periodic flow forcing under transient and asymptotic conditions. The system is investigated via both an Eulerian approach, based on evolution of the temperature field, and a Lagrangian approach, based on topological analysis of the thermal transport routes.

The Eulerian analysis reveals that the temperature evolution, after a short-lived initial phase, is dictated by an exponentially decaying transient mode superimposed upon an asymptotic mode, where the decay time varies only marginally with the flow forcing. The transient and asymptotic modes exhibit time-periodic evolution in case of time-periodic flow forcing that, following Fourier analysis, is dominated by a steady mode and one oscillatory mode. The fluid-wall heat transfer in both transient and asymptotic states depends basically only on the steady mode that, in turn, depends primarily on the relative strength of advection yet not on its nature. These findings imply that, in the present system, chaos is virtually ineffective for acceleration of the transient or fluid-wall heat-transfer enhancement. Moreover, they expose a counter-intuitive role in that chaos promotes heterogeneity instead of homogeneity.

The Lagrangian analysis reveals that chaotic heat transfer is spatially confined to the interior of the flow domain. Thermal transport near the (non-adiabatic) walls - and fluid-wall heat transfer - is for both steady and time-periodic conditions as well as in transient and asymptotic states determined by a thermal path connecting bottom and top walls. This path depends mainly on the relative strength of advection yet not on its nature, explaining the ineffectiveness of chaos for heat-transfer enhancement. The Lagrangian analysis furthermore reveals that temperature fluctuations emerge from the transition region between thermal path and chaotic zone. Thermal homogenisation happens via efficient "thermal mixing" by chaotic thermal trajectories in the core of said zone in essentially the same way as efficient fluid mixing. This explains why chaos promotes thermal heterogeneity near the bounding walls and thermal homogeneity in the domain interior.

The present study reveals that optimal thermal conditions are at lower Pe numbers not automatic with chaos and depend on a delicate (and highly non-trivial) interplay between flow and heat-transfer mechanisms. Further investigations on this matter are in progress.

REFERENCES

[1] T. Lemenand and H. Peerhossaini, 2002, "A thermal model for prediction of the Nusselt number in a pipe with chaotic flow", Appl. Thermal. Sci., Vol. 22, 1717.
[2] D.R Lester et al., 2009, "Low Reynolds number scalar transport enhancement in viscous and non-Newtonian fluids", Int. J. Heat Mass Transfer, Vol. 52, 655.
[3] A. Mokrani et al., 1997, "The effects of chaotic advection on heat transfer", Int. J. Heat Mass Transfer, Vol. 40, 3089.
[4] M.F.M. Speetjens et al., 2006, "Topological mixing study of non-Newtonian duct flows", Phys. Fluids, Vol. 18, 103103.
[5] B. Sundén and R.K. Shah, 2007, "Advances in Compact Heat Exchangers", Edwards, Philadelphia.
[6] L. Zaheed and R.J.J. Jachuck, 2004, "Review of polymer compact heat exchangers, with special emphasis on a polymer film unit", Appl. Therm. Engng, Vol. 24, 2323.
[7] D.J. Beebe et al., 2002, "Physics and applications of microfluidics in biology", Annu. Rev. Biomed. Engng, Vol. 4, 261.
[8] N.-T. Nguyen and Z. Wu, 2005 "Micro-mixers - a review", J. Micromech. Microengng, Vol. 15, R1.
[9] H.A. Stone et al., 2004, "Engineering flows in small devices: microfluidics toward a lab-on-a-chip", Ann. Rev. Fluid Mech., Vol. 36, 381.
[10] S. Cerbelli et al., 2004, "Eigenvalue-eigenfunction analysis of infinitely fast reactions and micromixing regimes in regular and chaotic bounded flows", Chem. Eng. Sci., Vol. 59, 2125.
[11] D.R. Sawyers et al., 1998, "Heat transfer enhancement in three-dimensional corrugated channel flow", Int. J. Heat Mass Transfer, Vol. 41, 3559.
[12] M. Giona et al., 2004 "Universality and imaginary potentials in advection–diffusion equations in closed flows", J. Fluid Mech., Vol. 513, 221.
[13] V.V. Meleshko and G.W.M. Peters, 1996, "Periodic points for two-dimensional Stokes flow in a rectangular cavity", Phys. Lett. A, Vol. 216, 87.
[14] M.F.M. Speetjens, 2008, "Topology of advective-diffusive scalar transport in laminar flows", Phys. Rev. E, Vol. 77, 026309.
[15] M.F.M. Speetjens and A.A. van Steenhoven, 2009, "A way to visualise laminar heat-transfer in 3D unsteady flows", Int. J. Thermal Sci. (in press).
[16] J.M. Ottino, 1989, "The Kinematics of Mixing: Stretching, Chaos and Transport", Cambridge University Press, Cambridge.
[17] S. Wiggins and J.M. Ottino, 2004, "Foundations of chaotic mixing", Phil. Trans. R. Soc. Lond. A, Vol. 362, 937.
[18] C. Canuto et al., 1987, "Spectral Methods in Fluid Dynamics", Springer, Berlin.